Title

NONEQUILIBRIUM THERMODYNAMIC THEORY FOR CONCENTRATION PROFILES IN LIQUID EXTRACTION

Authors

Hennico, Alphonse
Vermeulen, Theodore.

Publication Date

1960-09-30

UCRL 9415

UNIVERSITY OF
CALIFORNIA

Ernest O. Lawrence

Radiation Laboratory

NONEQUILIBRIUM THERMODYNAMIC THEORY FOR CONCENTRATION PROFILES IN LIQUID EXTRACTION

DISCLAIMER

UCRL-9415
UC-4 Chemistry - General
TID 4500 (15th Ed.)

UNIVERSITY OF CALIFORNIA

Lawrence Radiation Laboratory
Berkeley, California

Contract No. W-7405-eng-48

NONEQUILIBRIUM THERMODYNAMIC THEORY FOR CONCENTRATION PROFILES IN LIQUID EXTRACTION

Alphonse Hennico and Theodore Vermeulen

September 30, 1960

Printed in USA. Price $1.25. Available from the
Office of Technical Services
U. S. Department of Commerce
Washington 25, D.C.

Contents

NONEQUILIBRIUM THERMODYNAMIC THEORY FOR CONCENTRATION PROFILES IN LIQUID EXTRACTION

Alphonse Hennico and Theodore Vermeulen

Lawrence Radiation Laboratory
and Department of Chemical Engineering
University of California, Berkeley, California

September 30, 1960

ABSTRACT

The pattern or "profile" of concentration change in each of the two countercurrent streams, within a packed extraction column involving a three-component system, is generally assumed to follow either branch of the mutual-solubility curve for the system. In the work reported here, such concentration profiles have been computed for an idealized extraction process, and the profiles have been found to depart from the equilibrium curve.

The idealized extraction has the following characteristics: It involves a system with thermodynamically defined equilibrium behavior, rather than with known experimental behavior. Mass-transfer-coefficient ratios are held constant at any one steady-state condition of operation (called a "run") but are varied in different runs. A modified activity-gradient, derived both for molecular diffusion and for penetration-theory conditions, is postulated to govern mass-transfer and is used in place of the usual concentration driving potential.

The present calculations show that the concentration profile for the raffinate will usually be carried into a metastable condition, represented by a locus inside the equilbrium curve. The extract compositions always remain appreciably outside the equilibrium curve. Solute depletion, mainly, is found to explain the result for the raffinate phase, in much the same way that temperature lowering leads to supersaturation in binary solutions. Solute enrichment is the cause of the extract-phase behavior. The distance between the calculated concentration paths and the equilibrium curve depends on the values of the mass-transfer coefficients. Values of the number of transfer units

obtained from the exact concentration profiles can differ as much as 10% from the values given by the usual equilibrium-curve approximation.

INTRODUCTION

For ternary liquid systems undergoing countercurrent extraction in packed columns or other nonstaged equipment, calculation of the separation desired or obtained is often based upon the assumption that the composition of each coexisting phase lies on the mutual-solubility curve (S1, T1). By contrast, certain studies of mass-transfer rates between immiscible phases in binary systems have dealt entirely with the observable incompleteness of saturation in such systems, compared with the condition of equilibrium (C2, L1). It is also well known that in binary and multicomponent systems, a metastable range of compositions exists inside and adjacent to the mutual-solubility values, where nucleation will not occur spontaneously (G1, H1, K1, K2, P1). In this metastable region, diffusion to a second phase is believed to provide the sole mechanism by which the system can tend toward equilibrium. Thus it is possible, in principle, to encounter nonequilibrium compositions that may lie either inside or outside the equilibrium solubility curve.

In this paper we examine the pattern of deviations from the mutual-solubility curve, to assess the validity of the usual calculations and to see how the deviations can be related to the mass-transfer coefficients for the individual components. We will assume that the concentrations vary continuously from point to point, as in a packed column; also, that no longitudinal dispersion occurs, although this effect would not upset the qualitative conclusions that are found to apply in its absence.

The results obtained, which depend upon standard approaches to thermodynamics and to mass transfer, indicate in some cases that the concentration profile can penetrate into the metastable range. This conclusion, although plausible, has not been confirmed experimentally; to do so would require extremely accurate measurements. In case eventual experiments were to lead to a contrary conclusion, this would probably call for some modification of existing views on phase equilibrium and mass transfer.

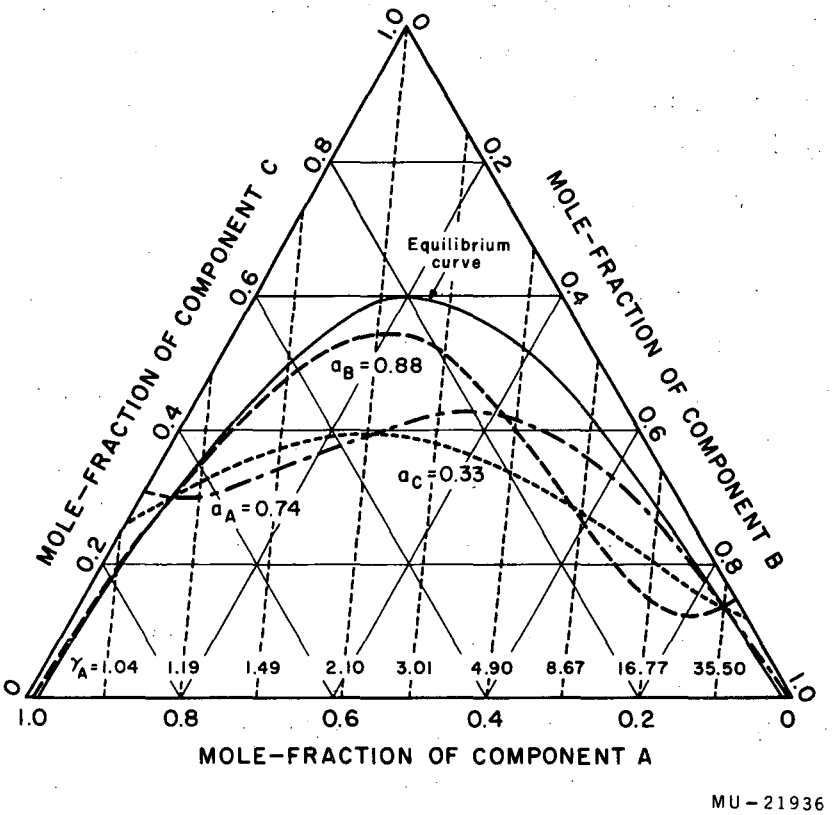

Fig. 1. Representative lines of constant-activity coefficients (γ_A) and constant activity (a_A, a_B, a_C).

THERMODYNAMIC BACKGROUND

In a nonelectrolyte system the thermodynamic activity of each component, in either phase of a two-phase system, is customarily expressed as a fraction of the activity of the corresponding pure component in the liquid state. Equilibrium is the condition in which the activity of each component is the same in both phases, corresponding to tie-line composition values whose locus forms the mutual-solubility curve. Figure 1 for a ternary system shows a set of activity contours, for the three components which participate in two three-way intersections and thus define the ends of an equilibrium tie-line. A study of such contours leads to the conclusion that points representing only partial equilibrium (i. e., equal activities of one, or two, components) must lie off the solubility curve; and that a single-phase ternary mixture has no thermodynamic "preference" for a solubility-curve composition.

Equations

Conclusions of a general type are sought in this investigation that will be independent of the particular calculation methods used. In order to obtain the greatest self-consistency, the ternary system to be treated is defined mathematically rather than by experiment. Activity-coefficient equations of simple form are used; for a binary pair AB, the form is:

$$\ln \gamma_A = A_{AB} x_B^2$$

and

$$\ln \gamma_B = A_{AB} x_A^2. \qquad (1)$$

For component A in a ternary mixture ABC, the relation becomes

$$\ln \gamma_A = f_A (x_A, x_B, x_C)$$

$$= A_{AB}x_B^2 + A_{AC}x_C^2 + (A_{AB} + A_{AC} - A_{BC})x_B x_C. \qquad (2)$$

In these equations, x is mole-fraction, γ is activity coefficient, A is a numerical constant, and f indicates a function.

The binodal (mutual-solubility) curve is then obtained by iterative simultaneous solution of three activity equations of the following type, one for each component:

$$(\ln a_A =);\ \ln x_{A1} + f_A(x_A, x_B, x_C)_1 = \ln x_{A2} + f_A(x_A, x_B, x_C)_2, \qquad (3)$$

where a is the activity, and subscripts 1 and 2 refer respectively to the two coexisting phases.

The spinodal curve, which separates the metastable from the unstable region (K1, P1), is given by

$$A_{AB}x_Ax_B + A_{AC}x_Ax_C + A_{BC}x_Bx_C + \frac{1}{2}(Mx_Ax_Bx_C - 1) = 0, \qquad (4)$$

with $M = (A_{AB} - A_{AC} - A_{BC})^2 - 4A_{AC}A_{BC}$. This curve becomes tangent to the mutual-solubility curve at one point only, the critical or plait point.

Application to a Typical Case

The idealized ternary system to be used is modeled after the system n-decane (A)/butadiene (B)/furfural (C), for which experimental data have been reported by Smith and Braun (S2). The binary constants selected are $A_{AC} = 0.7369$, $A_{BC} = 1.5376$, and $A_{AB} = 4.4100$. Because the square roots of these constants are additive (that is, $A_{AB}^{1/2} = A_{AC}^{1/2} + A_{AB}^{1/2}$), M is equal to zero, and all curves of constant activity coefficient are linear and parallel, as indicated in Fig. 1 and Table I. This type of additivity conforms to the Hildebrand solubility-parameter treatment of nonideal solutions (H4).

A two-phase ternary system is characterized by six concentrations. Of these, one (for instance, x_{C1}) can be taken as the independent variable. Two others (x_{A1} and x_{B2}) are eliminated by material balance. The remaining three are determined by solving three simultaneous equations, each having the form of Eq. (3). This set is most easily solved by repeated iteration, which lends itself to use on a digital computer. First, a trial set of concentration values is assumed and is used to evaluate the activity-coefficient terms (f's). The equation for a_C is then solved for x_{C2}, and the remaining equations are solved simultaneously for x_{B1} and x_{A2}. The results are used as a new trial set, and iteration is repeated until the results converge.

Table I. Activity coefficients for constant-coefficient lines

x_{B1} at $x_C = 0$	γ_C	γ_A	γ_B
0	2.09	1.00	82.27
0.1	1.54	1.04	35.51
0.2	1.21	1.19	16.77
0.3	1.05	1.49	8.67
0.41	1.00	2.10	4.65
0.50	1.04	3.01	3.01
0.6	1.17	4.90	2.05
0.7	1.45	8.67	1.49
0.8	1.95	16.77	1.19
0.9	2.88	35.51	1.04
1.0	4.66	82.27	1.00

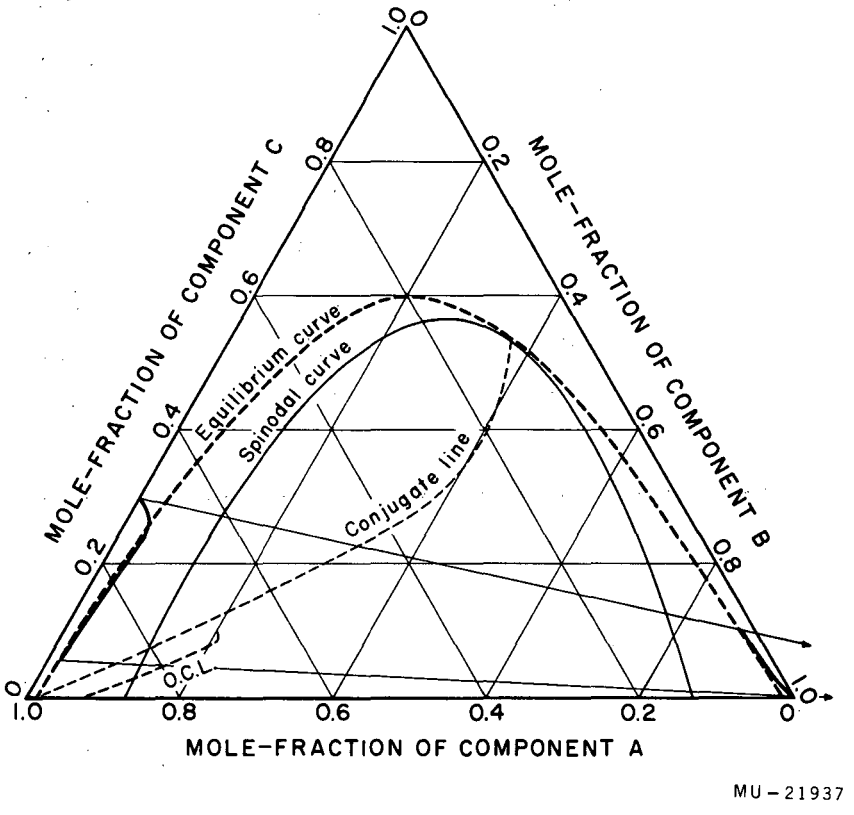

Fig. 2. Equilibrium diagram for idealized ternary system. Calculated concentration profiles shown for $k_{C2}/k_{C1} = 1$, $k_{B1}/k_{C1} = 1$, $k_{A2}/k_{C1} = 1$ with points related by the operating conjugate line (O. C. L.).

The equilibrium curve constructed in this manner is shown in Fig. 2; tie-line behavior is indicated by the usual type of conjugate line. For reference, the spinodal curve obtained from Eq. (4) is also shown. (The remaining curves of this figure will be described later.)

In order to interrelate activity and composition on the left-hand branch of the equilibrium curve, the numerical results for the latter were fitted to polynomial equations by linear regression. The equations used are:

$$x_{C1} = \alpha_{(1)} a_{C1} + \alpha_{(2)} a_{C1}^2 + \alpha_{(3)} a_{C1}^3 + \alpha_{(4)} a_{C1}^4 \qquad (5)$$

and

$$x_{B1} = \beta_{(1)} + \beta_{(2)} x_{C1} + \beta_{(3)} x_{C1}^2 + \beta_{(4)} x_{C1}^3 + \beta_{(5)} x_{C1}^4 + \beta_{(6)} x_{C1}^5, \qquad (6)$$

In order, the α values are 0.4955648, 0.4915600, -0.1345536, and 1.613432; the β's are 0.0135076, 0.0496642, 0.0347659, 0.532461, -1.336651, and 2.067078. When a value of a_{C1} is used for solving equations and the resulting compositions are then used in Eq. (2) or (3), the mean deviation between the input and output a_{C1} is 3×10^{-5} activity unit.

SCOPE OF THE MASS-TRANSFER CALCULATIONS

Comparative calculations are reported in this paper for a number of countercurrent extraction runs utilizing the ternary system just described. Most of these calculated runs involve identical feed and solvent concentrations, identical extents of extraction of the distributed component (C), and nearly identical flow rates. The mass-transfer ratios $(ka)_{C2}/(ka)_{C1}$, $(ka)_{B1}/(ka)_{C1}$, and $(ka)_{A2}/(ka)_{C1}$ are all held constant in any one run, and are varied separately in different runs to investigate their influence on the path of the extraction process.

The mass-transfer resistance in each phase is assumed to lie between the bulk of the phase and the portion closest to the interface. In this treatment, no further resistance is ascribed to the interface; that is, in each calculation, equilibrium is assumed to exist at the interface with the activity of each of the three components at that point having the same value in both phases.

The concentration paths followed by the two phases during each run have been calculated by a repetitive stepwise procedure, starting at either the feed end or the solvent end of the column. Assumed values of exit composition were varied with respect to carrier components A and B until the paths computed from the two directions agreed closely.

The equations used for these numerical calculations will be derived below, after a discussion of the mass-transfer relations on which the calculations were based.

DRIVING POTENTIAL FOR MASS TRANSFER

The "driving potential" for transfer between phases is usually defined in terms of the concentration gradient in the vicinity of the interface, based upon broad experience with situations where activity coefficients within a phase are essentially constant. In these terms the rate of mass transfer is

$$N_j = k'_{jp} (c_{jp} - c_{jip}), \tag{7}$$

where N is the number of moles of component j transferring per unit area per unit time under a steady-state concentration difference between the p-phase side of the interface and the bulk p phase, and k'_{jp} is the appropriate mass-transfer coefficient. In this treatment, concentrations will be replaced by mole fractions, with k_{jp} applying to these units.

Whenever the activity coefficient varies, however, a modified activity difference should replace the concentration difference, as a factor that indicates more accurately the direction and relative magnitude of material transfer. Such an activity difference is most nearly correct for molecular diffusion. Since material transfer between phases often involves the combined effect of molecular diffusion and eddy transport, the activity difference may provide only an improved approximation for the driving potential. Critical experimental tests to demonstrate the true mechanism are lacking.

Diffusion, as a molecular phenomenon, must depend upon the concentrations of molecules physically present. The activity difference can be expressed in units of concentration if it is divided by an appropriate mean activity coefficient. It thus reduces to the familiar concentration-difference form if the activity coefficient is constant along the mass-transfer path. Another intuitive argument in support of the activity-difference formulation has been given by Handlos and Baron (H2). These qualitative considerations can be replaced by the following formal derivations.

Molecular Diffusion

On the basis of absolute-rate theory, Stearn and Eyring (S3) have shown for binary systems that the rate of transfer of a component per unit area (N), uncorrected for bulk flow, is

$$N = -D_0 \frac{\eta_0}{\eta} \frac{d \ln a}{d \ln x} \frac{dx}{db}, \tag{8}$$

where D_0 is the diffusion coefficient at infinite dilution, η is the actual viscosity, η_0 is the viscosity at infinite dilution, a is the activity of the component, x is its mole fraction, and b is a length coordinate. A similar result has been given by Darken (D2), using a somewhat different basic method. The effect of the Stearn and Eyring derivation is that the activity-coefficient gradient slightly reduces the free energy of activation for diffusion in the direction of decreasing γ, and slightly increases it in the opposite direction. For our purposes, viscosity changes will be neglected, and the ratio η_0/η will be taken as unity. In an alternate form the rate is

$$N = -(D_0 \frac{x}{a}) \cdot \frac{da}{dx} \cdot \frac{dx}{db} = -\frac{D_0}{\gamma} \cdot \frac{da}{db}. \tag{9}$$

If the material transfer is examined in a single region, the rate N will be a constant across the "film" at any one level in an extraction tower. Hence, we can integrate by separation of variables:

$$N \int_0^B db = -D_0 \int_{a_i}^{a} \frac{da}{\gamma}. \tag{10}$$

For diffusion within a single phase, γ may be replaced by an appropriate average value, γ_m, which is constant at any one level. (If γ varies linearly with a, γ_m becomes the logarithmic mean.) This enables the relation to be written in integral form:

$$N = \frac{D_0}{B} \cdot \frac{1}{\gamma_m} (a - a_i). \tag{11}$$

We obviously wish to select a mass-transfer coefficient that will be as nearly constant as possible. If the "film" coefficient is taken to be $k = \frac{D_0}{B}$, then we have

$$N = \frac{k}{\gamma_m} (a - a_i). \tag{12}$$

For our ternary system, this will be generalized to give

$$N_j = \frac{k_{jp}}{\gamma_{jpm}} (a_{jp} - a_{jip}). \tag{13}$$

Thus the use of Eq. (13) can be supported on theoretical grounds. Whether or not it is completely accurate, it appears preferable to Eq. (7).

An alternate approach favored by some investigators, among them Opfell and Sage (O1), involves the use of a thermodynamic-potential gradient:

$$N = -\mathcal{D} \frac{d\mu}{db}. \tag{14}$$

Since the thermodynamic potential μ is given by $\mu = RT \ln a +$ constant, Eq. (14) leads to

$$N = -\frac{\mathcal{D}RT}{a} \frac{da}{db} = -\frac{1}{\gamma} \left(\frac{\mathcal{D}RT}{x} \right) \frac{da}{db}. \tag{15}$$

The coefficient $\mathcal{D}RT/x$ thus replaces D_0. In view of the molecular models of diffusion, it is much more likely that D_0 (rather than $\mathcal{D}$) is bassically a constant. The essential feature which this approach has in common with the preceding one is the determining effect of the activity-gradient driving potential.

Turbulent Diffusion

One can assume that a coupled process could occur, such that dissipation of mechanical energy would perturb the simple thermodynamic result, but it is extremely unlikely that such perturbation would regularly convert Eq. (13) to Eq. (7). Such a coupled process would lead to the following equation for the mass transfer:

$$N_A = \frac{k_{Ap}}{\gamma_{Apm}} (a_{Ap} - a_{Aip}) + k'_{Ap}(c_{Ap} - c_{Aip}), \qquad (16)$$

probably with $k'_{Ap} << k_{Ap}$. Hence the factor due to dissipation of mechanical energy should play a minor role.

Such a coupled process, considered in terms of Eq. (16), provides the following conclusions:

(a) for $da/dx = 0$ and $dc/dx \neq 0$, material transfer may occur in the direction indicated by Δc.

(b) For $dc/dx = 0$ and $da/dx \neq 0$, it is virtually certain that material transfer occurs in the direction indicated by Δa.

(c) In the intermediate case, for $dc/dx > 0$ and $da/dx < 0$, Δa would generally govern, because of the above assumption.

The penetration theory relates turbulent diffusion to molecular diffusion in certain cases (H3, D1). By a procedure analogous to the usual development (in terms of concentration driving potential) of Fick's second law from his first law, Eq. (9) can be shown to yield

$$\frac{\partial x}{\partial t} = \frac{D_0}{\gamma} \frac{\partial^2 a}{\partial b^2} \quad . \qquad (17)$$

Introducing the relation between activity and concentration, we find that

$$\frac{\partial x}{\partial t} = \frac{\partial a}{\partial t} \cdot \frac{1}{\gamma \left(\frac{\partial \ln a}{\partial \ln x}\right)} \quad . \qquad (18)$$

From Eqs. (17) and (18), with $\partial \ln a / \partial \ln x$ taken to be a constant at its mean value, we can derive the approximate result

$$\frac{\partial a}{\partial t} = D \frac{\partial^2 a}{\partial b^2} , \tag{19}$$

where

$$D = \left(\frac{\partial \ln a}{\partial \ln x}\right)_m D_0. \tag{20}$$

With the introduction of suitable initial and boundary conditions, the solution of Eq. (19) becomes

$$\frac{a - a_b}{a_i - a_b} = \text{erf} \frac{b}{2\sqrt{Dt}} , \tag{21}$$

with a_b and a_i as the bulk and interface activity values, and erf representing the error function as defined by the relation

$$\text{erf } V = \frac{2}{\sqrt{\pi}} \int_0^V e^{-z^2} dz. \tag{22}$$

The amount of material diffusing through the interface is equal to

$$N = - \frac{D_0}{\gamma} \left(\frac{\partial a}{\partial b}\right)_{b=0} \tag{23}$$

or

$$N = -\sqrt{\frac{D_0}{\pi t}} \frac{a_i - a_b}{\gamma_i \left(\frac{\partial \ln a}{\partial \ln c}\right)_m^{1/2}} . \tag{24}$$

By defining a new diffusion coefficient

$$D' = \frac{D_0}{\left(\frac{\partial \ln a}{\partial \ln c}\right)_m} , \tag{25}$$

we can rewrite Eq. (21) as

$$N = \sqrt{\frac{D'}{\pi t}} \frac{a_b - a_i}{\gamma_i} . \tag{26}$$

This result has the important significance that, in the particular case corresponding to the penetration-theory model, the direction of the activity gradient is shown to govern the direction of turbulent diffusion

as well as that of molecular diffusion. By assuming as before that $\gamma_i = \gamma_m$, we observe in Eq. (26) that the effective mean activity coefficient is an essential factor in relating the activity driving potential to the rate of mass transfer.

On the assumption that the results derived for a binary system also apply to a ternary, the correction factor introduced in Eq. (25) has been evaluated for the ternary system under consideration in a few representative instances, which are shown in Table III. This is derived from a calculated run that is summarized in Table II (to be explained below). The correction, which would enter the mass-transfer coefficient as a square root, varies appreciably from a constant value, but the extreme variation lies within a factor of two. Since this range of variation would not affect the qualitative conclusions to be drawn from this study, the molecular-diffusion relation of Eq. (13) has been used instead of the penetration-theory result of Eq. (26), as the basis of our calculations.

As a qualitative conclusion, the rarely encountered case where the activity gradient opposes the concentration gradient can be handled most correctly by using an activity gradient as the driving potential. For the usual case, where the two gradients are concurrent, the choice of driving potential is less critical from the calculational standpoint, but the activity gradient still seems to be much preferred on theoretical grounds.

Multigradient Effects

For precise calculations on a ternary system, another type of coupling that must be considered is the cross-product transport which results from diffusion of the other species. The formulations of irreversible thermodynamics (D3, G2) suggest complete equations of the type

$$N_A = \frac{k_{AAP}}{\gamma_{Apm}} (a_{Ap} - a_{Aip}) + \frac{k_{ABp}}{\gamma_{Bpm}} (a_{Bp} - a_{Bip}) + \frac{k_{ACp}}{\gamma_{Cpm}} (a_{Cp} - a_{Cip})$$

$$= \frac{k_{Ap}}{\gamma_{Apm}} (a_{Ap} - a_{Aip}). \qquad (27)$$

Table II. Activity coefficients during extraction into phase 2 [a]

Location	X_{C1}	X_{C1i}	X_{C2i}	X_{C2}	γ_{C1}	γ_{C1i}	γ_{C2i}	γ_{C2}	a_{C1}	a_{Ci}	a_{C2}
1	0.09500	0.07500	0.03426	0.01377	1.714	1.777	3.892	4.300	0.1628	0.1333	0.0592
2	0.17409	0.15000	0.06821	0.04481	1.529	1.593	3.504	3.821	0.2663	0.2390	0.1712
3	0.24739	0.22500	0.10223	0.07761	1.400	1.438	3.165	3.444	0.3465	0.3236	0.2673
Location	X_{B1}	X_{B1i}	X_{B2i}	X_{B2}	γ_{B1}	γ_{B1i}	γ_{B2i}	γ_{B2}	a_{B1}	a_{Bi}	a_{B2}
1	0.02105	0.01765	0.95060	0.97913	49.263	54.159	1.006	1.001	1.0374	0.9560	0.9800
2	0.02779	0.02300	0.91486	0.94251	35.825	40.307	1.013	1.007	0.9956	0.9274	0.9489
3	0.03176	0.03027	0.87884	0.90728	27.505	29.855	1.028	1.016	0.8736	0.9038	0.9222
Location	X_{A1}	X_{A1i}	X_{A2i}	X_{A2}	γ_{A1}	γ_{A1i}	γ_{A2i}	γ_{A2}	a_{A1}	a_{Ai}	a_{A2}
1	0.88395	0.90735	0.01514	0.00710	1.016	1.010	60.553	72.028	0.8980	0.9167	0.5114
2	0.79812	0.82700	0.01693	0.01268	1.044	1.032	50.407	58.659	0.8334	0.8534	0.7438
3	0.72085	0.74473	0.01893	0.01511	1.081	1.068	42.028	48.855	0.77939	0.7956	0.7382

[a] $(X_{C1})_{initial} = 0.30$; $k_{C2}/k_{C1} = 1$; $k_{B1}/k_{C1} = 1$; $k_{A2}/k_{C1} = 1$ (Run 1)

Table III. Correction factor for penetration-theory equation

Location	$\left(\frac{\delta \ln a_C}{\delta \ln X_{C1}}\right)$	$\left(\frac{\delta \ln a_C}{\delta \ln X_{C2}}\right)$	$\left(\frac{\delta \ln a_B}{\delta \ln X_{B1}}\right)$	$\left(\frac{\delta \ln a_B}{\delta \ln X_{B2}}\right)$	$\left(\frac{\delta \ln a_A}{\delta \ln X_{A1}}\right)$	$\left(\frac{\delta \ln a_A}{\delta \ln X_{A2}}\right)$
1	0.857	0.832	0.528	0.730	0.812	0.765
2	0.790	0.803	0.376	0.770	0.669	0.467
3	0.721	0.692	0.706	0.634	0.631	0.332

Theoretically, then, the partial coefficients k_{AAp}, k_{ABp}, and k_{ACp} will be essentially constant, and the apparent coefficient k_{Ap} which results will vary. In practice, the cross-product coefficients k_{ABp} and k_{ACp} may be small compared to k_{AAp}, and thus $k_{AAp} \approx k_{Ap}$. Professor Raymond Defay, of the University of Brussels, has suggested that the cross-product terms can be viewed physically as representing a type of entrainment.

Mean Activity Coefficient

The activity difference must be corrected to mole-fraction (or concentration) units by being divided by the effective mean activity coefficient. In our calculations, the mean values were not known initially, and could only be obtained iteratively by beginning the calculation with assumed values.

In order to simplify the computation, this iteration was omitted, and the mean activity coefficient in each phase (γ_m) was replaced by the value of this coefficient (γ) in the bulk phase. The error introduced in the rate of mass-transfer of any one component never exceeded 10% in any step, and was usually under 5%. Such an error is equivalent to this magnitude of variation in the mass-transfer coefficients. Representative values of γ and γ_i are shown for comparison in Table II. In this range, the arithmetic mean would be used for γ_m. Since we are concerned with evaluating the effects of gross changes in the ratios of k's (changes by a factor of two, or more), the error introduced by using γ for γ_m are not significant for the purposes of this investigation.

Although the mass-transfer coefficients (and their ratios) will probably not be exactly constant throughout an actual experimental run, the extent of increase or decrease in each k value will be a specific effect for the particular experimental conditions. The k values for the runs calculated in this study have been taken as constant, because no better general assumption could be made. The curves developed herein for constant k should be an aid in estimating the direction and extent of changes in k in actual experimental runs.

CALCULATION OF PROFILES

Degrees of Freedom for the Calculation

It is useful at this point to determine the number of parameters which will need to be specified in order to complete the calculations of any one incremental slice of column. The number of variables and parameters (a total of 53) as summarized in Table IV, is nine mass-transfer coefficients (three for each phase and three for the interface); six bulk concentrations and six activities at the start of the slice; six interfacial concentrations and six interfacial activities; six bulk concentrations and six activities at the end of the slice; two initial flowrates, two resultant flowrates; three component transfer rates; and the height of the slice.

These variables are related by several equations. In each phase and at the interface, the concentrations of some one component is related to the others by a simple material balance. From a knowledge of the concentrations, the activities can be computed by equations similar to Eq. (2). By the assumption that the interface is in equilibrium, we can eliminate the three mass-transfer coefficients corresponding to the interface, and reduce the number of interfacial variables from four to one. As other relations we have the usual column material-balances between concentrations and flowrates. Finally, we can write six mass-transfer equations like Eq. (26).

We thus have 11 independent variables to specify in order to solve the problem. As is usually necessary in solvent-extraction column calculations, we have first specified the concentrations and flowrates at one end of the column. As the remaining independent variables, we have elected to choose Δn_c (which we define indirectly through an approximate value of Δx_c) and four mass-transfer coefficients. Our purpose is not to calculate an absolute column height, but rather to determine the amounts of transfer of components A and B accompanying any given transfer of component C; therefore we have used three ratios of k's rather than four individual values.

By comparing the number of unknowns with the number of relations, it is easy to see that we could not specify either fewer or

Table IV. Variables and parameters for stepwise calculations

Variables and parameters	Initially	After material balance within phase	After activity equations (Eq. 2)	After equilibrium specification (Eq. 3)	After material balance within column	After six mass-transfer equations
Mass-transfer coefficients (k)	9	9	9	6	6	4
Initial bulk concentrations (x)	6	4	4	4	4	4
Initial bulk activities (a)	6	6	0	0	0	0
Interface concentrations (x_i)	6	4	4	1	1	0
Interface activities (a_i)	6	6	0	0	0	0
Resulting bulk concentrations (x')	6	4	4	4	0	0
Resulting bulk activities (a')	6	6	0	0	0	0
Initial flowrate (F)	2	2	2	2	2	2
Resulting flowrate (F')	2	2	2	2	0	0
Rate of transfer of component (Δn)	3	3	3	3	3	1
Height of slice (Δh)	1	1	1	1	1	0
Total	53	47	29	23	17	11

more than three ratios without under- or over-specifying the problem. In this study, we considered phase 1 and phase 2 as infinite reservoirs for the diffusion of A and B, respectively; thus, k_{A1}/k_{C1} and k_{B2}/k_{C1} were chosen as the dependent variables, the specified ones being k_{C2}/k_{C1}, k_{A2}/k_{C1}, and k_{B1}/k_{C1}.

As was explained in an earlier paragraph, it would be possible to include the cross-product transport in the mass-transfer equations (Eqs. 13 and 27). Thus we would get 12 mass-transfer coefficients (six more being eliminated by the Onsager reciprocal relations) and would have to specify ten instead of four. If the variables left unspecified were k_{AA1} and k_{BB2}, the calculations (although substantially more complex) would proceed very much as the present case. If any cross-product terms were left unspecified, several equations would need to be solved simultaneously. It seems likely that any assignment of coefficients that caused the unassigned factors to take on negative values would represent a physically unobtainable situation. Because correlation of column behavior in terms of the adjustable coefficients (or nine ratios) is a much more complex undertaking than one based on three ratios, the latter course was selected for this investigation.

Calculation Procedure

For a differential section of the column with unit cross-sectional area, the mass-transfer of each component between immiscible phases in countercurrent flow can be expressed by

$$dn_j = d(F_1 x_{j1}) = d(F_2 x_{j2}), \tag{28}$$

where F is the flowrate of the phase in moles per unit time, x is mole-fraction, and n is number of moles transferred from phase 2 to phase 1. Also, we have

$$dn_j = (ka)_{j1} \text{ (driving potential in phase 1 towards phase 1) } dh$$

$$= (ka)_{j2} \text{ (driving potential in phase 2 towards phase 1) } dh. \tag{29}$$

Here (ka) is the product of the mass-transfer coefficient and interfacial area per unit volume, and dh is the height of the differential section.

For small finite increments, for component A in phase 1, we can write

$$\Delta n_A = \Delta(F_1 x_{A1}) = (ka)_{A1}(x_{A1} - \frac{a_{Ai}}{\gamma_{A1}})\Delta h. \qquad (30)$$

Similar equations can be derived for components B and C, and for phase 2.

To begin the calculations of any one extraction step, we assume

$$\Delta n_C = F_1 \Delta x_{C1}, \qquad (31)$$

with Δx_{C1} taken as a convenient and uniform small interval (negative for calculations starting at the feed end; positive for those starting at the solvent end.) The relative height of column required for this transfer is then given by the expression:

$$(ka)_{C1}\,\Delta h = \frac{\Delta n_C}{\frac{a_{Ci}}{\gamma_{A1}} - x_{C1}} \quad . \qquad (32)$$

The driving potentials that apply at the start of each increment will be assumed to remain constant through the whole increment.

The value of a_{Ci} being unknown, it must be eliminated between the rate terms for component C in phases 1 and 2:

$$\frac{(ka)_{C1}(a_{C1} - a_{C1i})}{\gamma_{C1}} = \frac{(ka)_{C2}(a_{C2i} - a_{C2})}{\gamma_{C2}} \quad . \qquad (33)$$

With C in equilibrium at the interface, we have $a_{C1i} = a_{C2i} = a_{Ci}$, and Eq. (33) gives

$$a_{Ci} = \frac{a_{C1}\frac{(ka)_{C1}}{(ka)_{C2}} + \frac{\gamma_{C1}}{\gamma_{C2}}a_{C2}}{\frac{\gamma_{C1}}{\gamma_{C2}} + \frac{(ka)_{C1}}{(ka)_{C2}}} \quad . \qquad (34)$$

By using Eq. (32), we can then determine the relative height of column directly from this value of a_{Ci}. By use of relations of the form of Eq. (30), Δn_A and Δn_B are determined. The respective relations are

$$\Delta n_A = \frac{(ka)_{A2}}{(ka)_{C1}} \left(x_{A2} - \frac{a_{Ai}}{\gamma_{A2}} \right) (ka)_{C1} \Delta h \tag{35}$$

and

$$\Delta n_B = \frac{(ka)_{B1}}{(ka)_{C1}} \left(\frac{a_{B1}}{\gamma_{B1}} - x_{B1} \right) (ka)_{C1} \Delta h. \tag{36}$$

The ratios $(ka)_{A1}/(ka)_{C1}$ and $(ka)_{B2}/(ka)_{C1}$ are specified as constant values throughout any one run, and $(ka)_{C1} \Delta h$ is the relative height calculated from Eq. (32).

Then, over the increment, we have

$$(F_1)_{end} = (F_1)_{start} + \Sigma(\Delta n_j), \tag{37}$$

$$(n_{j1})_{end} = (n_{j1})_{start} + \Delta n_{j1}, \tag{38}$$

and

$$(x_{j1})_{end} = (n_{j1})_{end}/(F_1)_{end}. \tag{39}$$

Similar relations apply to phase 2. These last equations complete the calculation for any one step.

We can eliminate the inaccuracies resulting from nonconstant driving potentials within each step by repeating the calculation of an entire column with a smaller trial value of Δx_{C1}; increments of 0.005 mole-fraction of C, or in some cases 0.0025, sufficed to give a satisfactory convergence.

Results

The results of the stepwise calculations are reported in Figs. 2 through 6, which record the concentration path followed by each phase inside the column, with reference to the equilibrium curve for that phase.

In Fig. 2, the calculated pair of concentration profiles for $k_{C2}/k_{C1} = 1$; $k_{B1}/k_{C1} = 1$; $k_{A2}/k_{C1} = 1$ already mentioned (a "1-1-1" run)

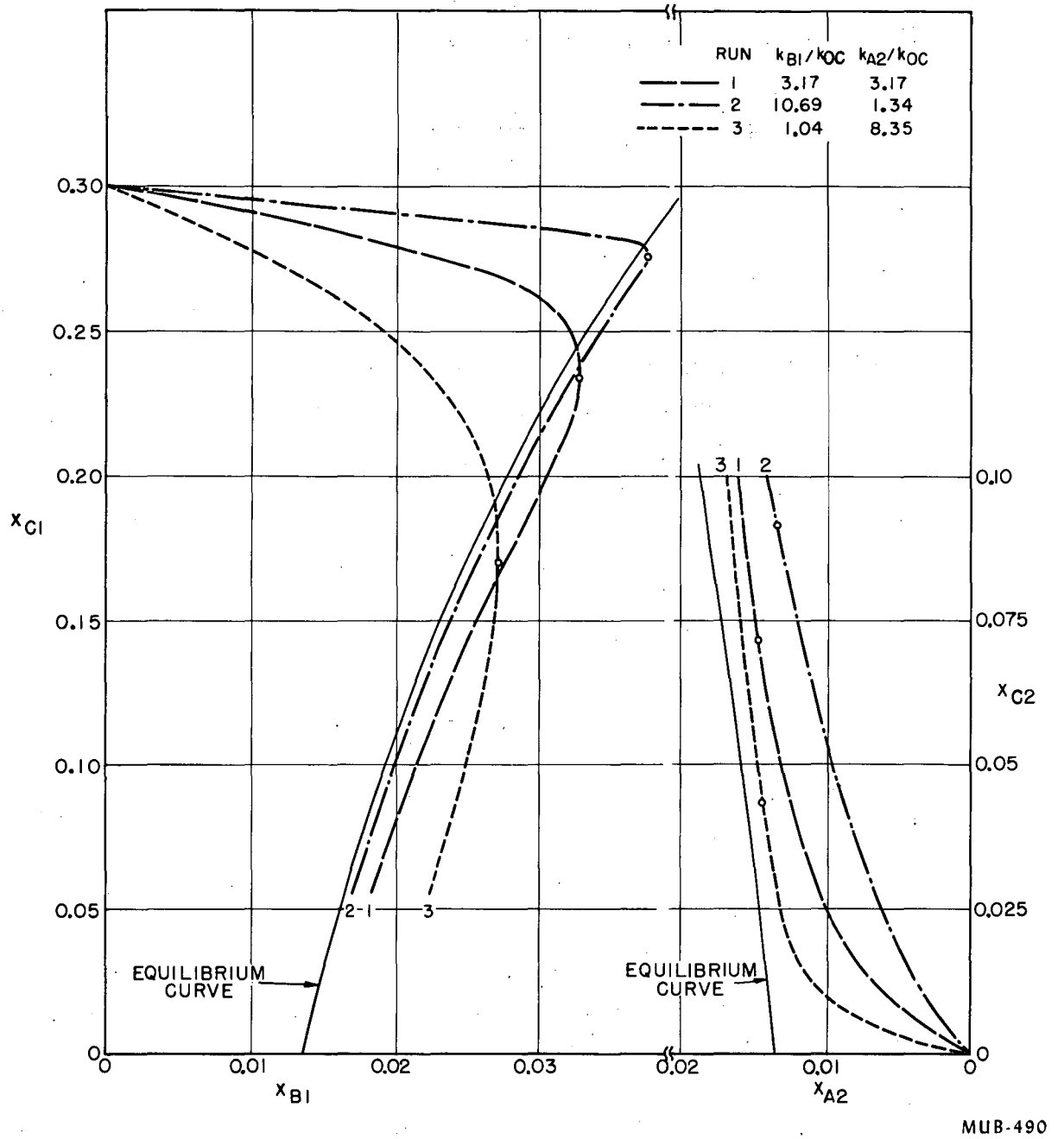

Fig. 3. Calculated concentration profiles showing the effect of the k_{B1}/k_{C1} ratio.

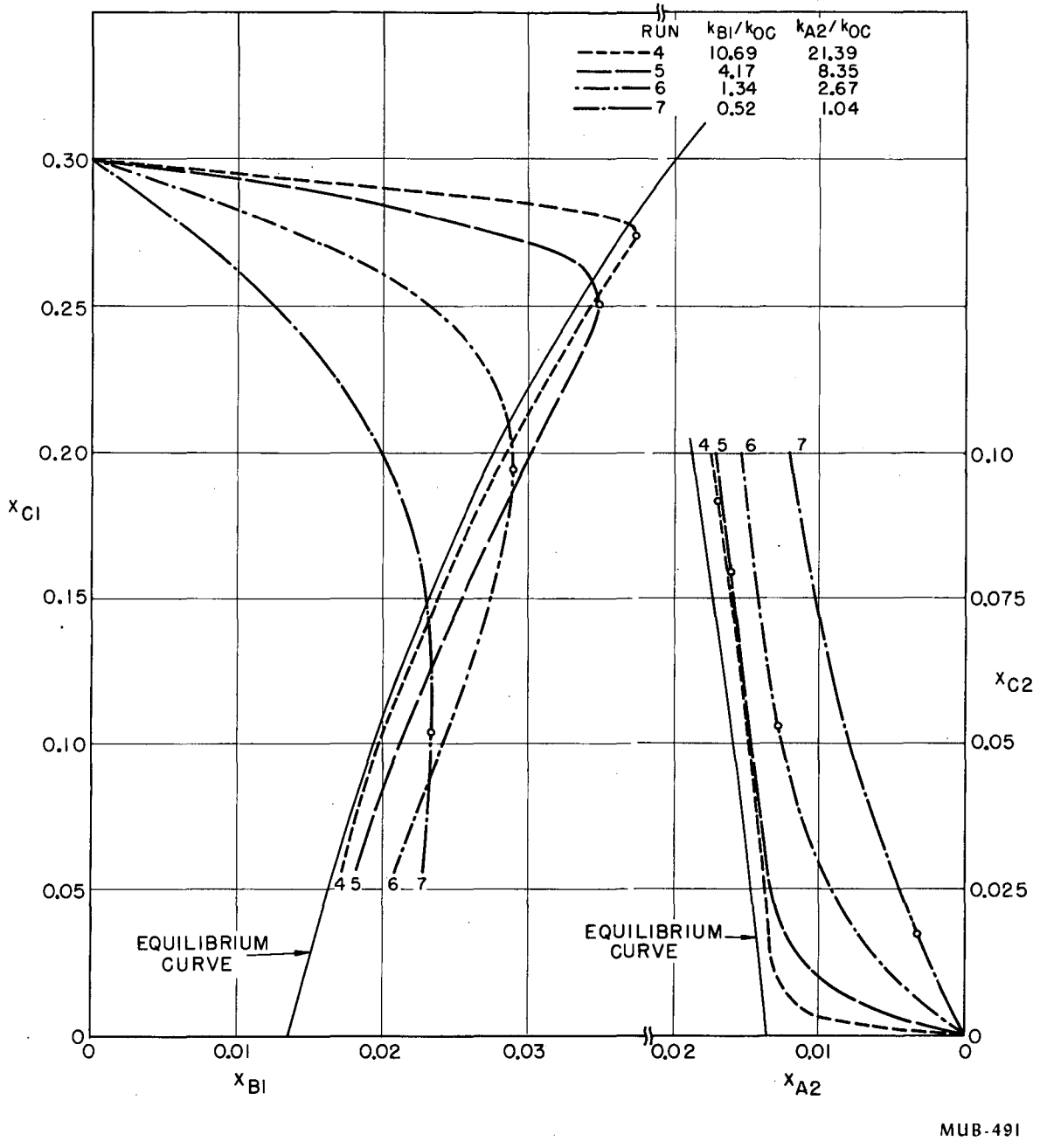

Fig. 4. Calculated concentration profiles showing the effect of the k_{B1}/k_{OC} and k_{A2}/k_{OC} ratios.

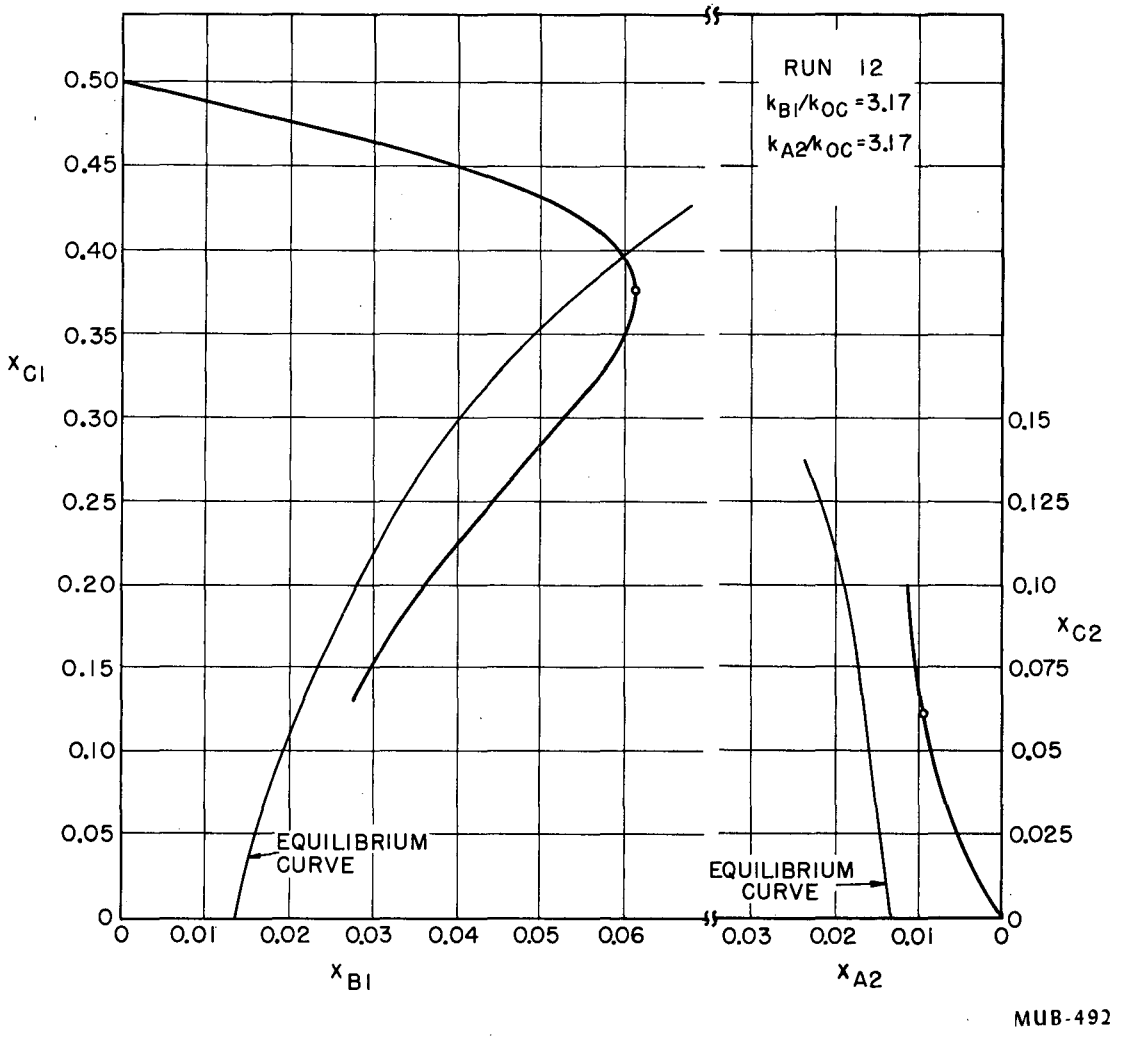

Fig. 5. Calculated concentration profile for a feed with higher concentration of C.

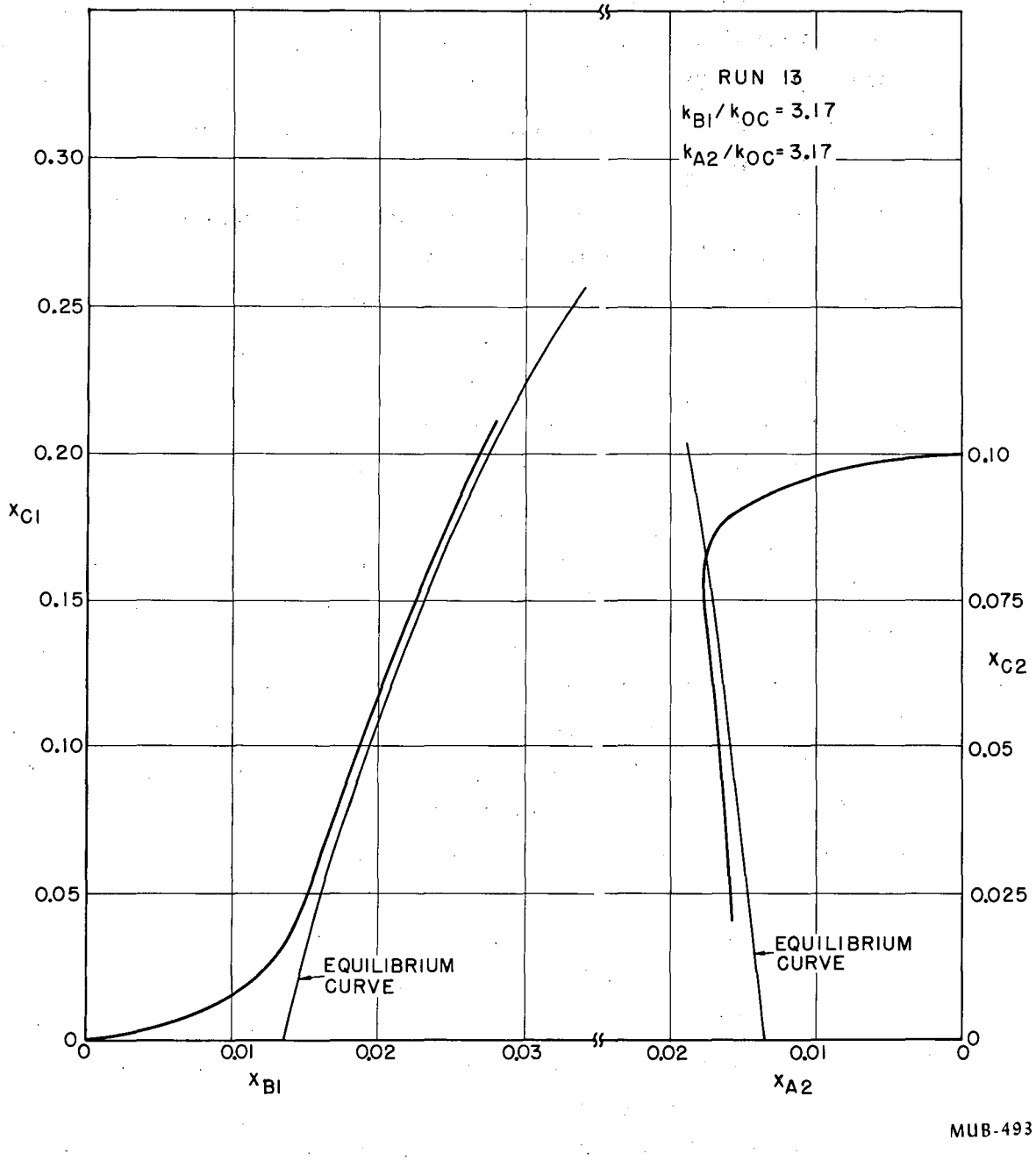

Fig. 6. Concentration profile for reverse extraction.

is plotted on the triangular graph. Lines are projected through co-existing points of the concentration path to form an operating conjugate line (O. C. L.), as well as the usual operating point (off the plot, to the right). The scale of the triangular plot conceals the difference between the actual profile and the equilibrium curve.

Rectangular coordinates allow greater flexibility in choice of scales, and thus provide a clearer view of the concentration-profile behavior. Most calculations are made for the case where the distribution component C is extracted from phase 1 into phase 2.

Figure 3 shows, as Run 1, the "1-1-1" run from Fig. 2. Two other runs are shown, for which k_{B1}/k_{C1} and k_{A2}/k_{C1} vary in opposite directions. To give an idea of the coexisting points in each run, the height in the column corresponding to the "knee" of the phase-1 curve is identified by a point on each of the two curves for the run.

Figure 4 shows a series of runs, for which k_{B1}/k_{C1} and k_{A2}/k_{C1} are always on the same side of unity; again the "knee" points are identified. In both figures it is seen that the concentration path followed by the three components falls partly inside the equilibrium curve for phase 1 but stays outside for phase 2. This crossing-over is quite general and occurs whatever k ratios were chosen. The rapidity with which each concentration profile approaches the respective equilibrium curve depends largely on the k ratios, and will be discussed in a later paragraph.

The concentration profiles for the two phases behave somewhat independently. In Fig. 3 the run that lies farthest inside the two-phase region for phase 1 (Run 3) is nearest the equilibrium curve for phase 2, but in Fig. 4 the run that is farthest on one side is also the farthest on the other (Run 7).

Another interesting feature observed in this study is that the calculations for curves that approach the equilibrium line very rapidly on the phase-1 side (Run 2, for Fig. 3; Run 4 for Fig. 4) have an unstable behavior. That is, for such runs, the terminal mole-fractions used as input to the stepwise calculations were fixed to the nearest integer in the last place of eight significant figures, and still only

bracketed the results of the oppositely-directed calculation rather than converging exactly upon a single curve.

In addition to the runs shown in Figs. 3 and 4, four calculations were made (Runs 8 through 11) with still other sets of mass-transfer coefficients. Since the results are similar to and consistent with those shown in Figs. 3 and 4, they are not plotted separately. However, all these calculations are summarized in Table V. The nearness with which equilibrium is approached as a stream leaves the column is indicated by the outlet $(x_A)_2$ and $(x_B)_1$ values; at equilibrium these would be respectively 0.01878 (precisely) and 0.0165 (approximately, due to small variations in the outlet value of $(x_C)_1$).

Two other extraction runs calculated with unit ratios of the mass-transfer coefficients (hence, "1-1-1" runs) are also listed in Table V. Figure 5 shows the concentration path for a feed richer in C(x_{C1} = 0.50), calculated with a correspondingly higher relative flow-rate for phase 2. Again the crossing-over occurs for phase 1 but not for phase 2. Figure 6 shows a "reverse" extraction at essentially the same feed-rate ratio used in most of the "forward" calculations. For interpreting the result of the calculations, it is significant that the concentration path for this reverse run crosses the equilibrium curve for phase 2 but not for phase 1.

Table V. Summary of calculated extraction runs, showing mass-transfer coefficients and terminal concentrations

Run No.	k_{C2}/k_{C1}	k_{B1}/k_{C1}	k_{A2}/k_{C1}	k_{0C}/k_{C1}	k_{B1}/k_{0C}	k_{A2}/k_{0C}	k_{A1}/k_{C1} upper x_C	k_{A1}/k_{C1} knee	k_{A1}/k_{C1} lower x_C	k_{B2}/k_{C1} upper x_C	k_{B2}/k_{C1} extreme	k_{B2}/k_{C1} lower x_C	$(x_C)_1$ out	$(x_B)_1$ out	$(x_C)_2$ out	$(x_A)_2$ out
9[a]	0.5	4.0	2.0	0.187	21.39	10.69	-0.035	-0.074	-2.418	+3.888	-0.064	-0.031	0.05655	0.01698	0.1000	0.01722185
2	0.5	2.0	0.25	0.187	10.69	1.34	-0.025	-0.092	-0.302	+1.841	-0.053	-0.023	0.05592	0.01699	0.1000	0.014200
4	0.5	2.0	4.0	0.187	10.69	21.39	-0.054	-0.071	-4.700	+1.940	-0.063	-0.035	0.05652	0.01723	0.1000	0.0171146
11	2.0	4.0	2.0	0.479	8.35	4.17	-0.215	-0.076	-0.938	+6.083	-0.234	-0.091	0.05648	0.01738	0.1000	0.016990
5	2.0	2.0	4.0	0.479	4.17	8.35	-0.179	-0.074	-1.833	+3.075	-0.221	-0.101	0.05650	0.018174	0.1000	0.017292
1	1.0	1.0	1.0	0.315	3.17	3.17	+0.075	-0.075	-0.680	+1.132	-0.093	-0.051	0.056233	0.018339	0.1000	0.016222
8	0.5	0.5	0.25	0.187	2.67	1.34	+0.029	-0.097	-0.270	+0.457	-0.041	-0.026	0.05576	0.018427	0.1000	0.01380
6	0.5	0.25	0.50	0.187	1.34	2.67	+0.026	-0.087	-0.680	+0.235	-0.034	-0.028	0.055984	0.02072	0.1000	0.015492
10	2.0	0.5	0.25	0.479	1.04	0.52	-1.926	-0.088	-0.107	+0.583	-0.091	-0.091	0.05458	0.02167	0.1000	0.008855
3	2.0	0.5	4.0	0.479	1.04	8.35	-0.392	-0.062	-1.657	+0.762	-0.146	-0.100	0.05620	0.02240	0.1000	0.017035
7	2.0	0.25	0.5	0.479	0.52	1.04	-1.990	-0.161	-0.208	+0.322	----	-0.053	0.05518	0.02260	0.1000	0.01215
12[b]	1.0	1.0	1.0	0.315	3.17	3.17	+0.485	-0.091	-0.305	+0.600	-0.132	-0.090	0.13092	0.027418	0.1000	0.011630
13[c]	1.0	1.0	1.0	0.315	3.17	3.17	+1.887	-0.057	-0.024	-0.067[d] +1.560[d] -0.315 +0.074		+0.778	0.21000	0.027725	0.02105	0.015770

[a] $(x_C)_{1,\,in} = 0.30$; $(x_A)_{1,\,in} = 0.70$; $(x_B)_{2,\,in} = 1.00$.

[b] $(x_C)_{1,\,in} = 0.50$; $(x_A)_{1,\,in} = 0.50$; $(x_B)_{2,\,in} = 1.00$.

[c] $(x_A)_{1,\,in} = 1.00$; $(x_C)_{2,\,in} = 0.10$; $(x_B)_{2,\,in} = 0.90$.

[d] Two sides of a discontinuity.

DISCUSSION

Crossing of the Equilibrium Curve

In order to explain this crossing of the equilibrium curve several factors must be considered. The crossing is not due solely to flow conditions, because at constant relative flow-rate the crossing depends on the direction of extraction. It is more correct to say that the effect is due to a nonequilibrium which is produced by the flow. Two principal factors must be considered: the effect of depletion (or enrichment) of component C, and the activity behavior of the minor component in each phase.

Depletion (or enrichment) of C. When the composition reaches the equilibrium line for phase 1 in the forward runs, the driving potential for B is close to zero and the rate of transfer of A is around one-tenth that of C. As already indicated, each phase of the system is characterized by its respective activities which in themselves do not provide any abrupt indication that the composition has reached or crossed the equilibrium curve. Thus the behavior of the phase depends mainly upon the relatively large rate of depletion of C (in the forward case). The equilibrium curve has a shallower slope than the line of constant A/B ratio. Since the A/B ratio varies quite slowly, this depletion (in the forward case) tends to pull the composition inside the curve (see Fig. 7a).

For phase 2 in the forward case, enrichment of C provides the major effect. In this phase, this enrichment carries the concentration path away from the equilibrium line and thus keeps it from crossing (Fig. 7b).

For the reverse case, the opposite situation is encountered; the depletion effect of C in phase 2 carries the concentration path across the equilibrium curve, and the enrichment effect of C in phase 1 pulls it away from it.

Activity effects. From the slope of the constant-activity lines, it appears quite certain that no transfer of B from phase 1 (or of A from phase 2 in the reverse case) will occur until the composition is appreciably inside the equilibrium line. In the forward case, the activity gradient for B in phase 1 changes in sign soon after phase 1 crosses

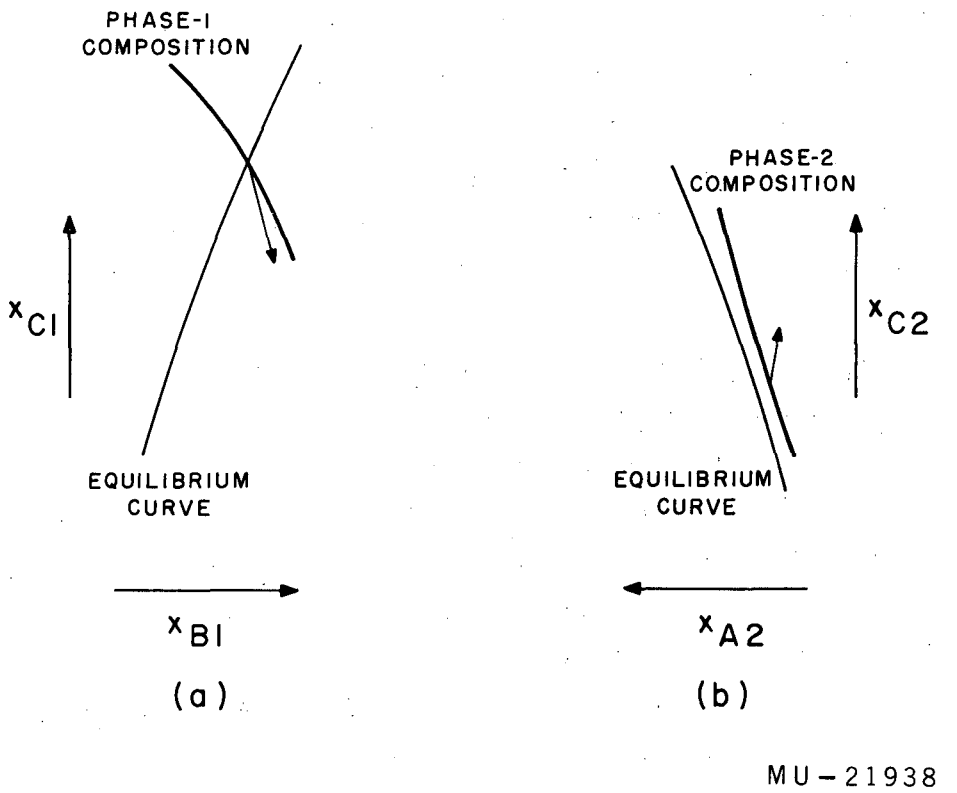

Fig. 7. Depletion and enrichment effects for compound C.

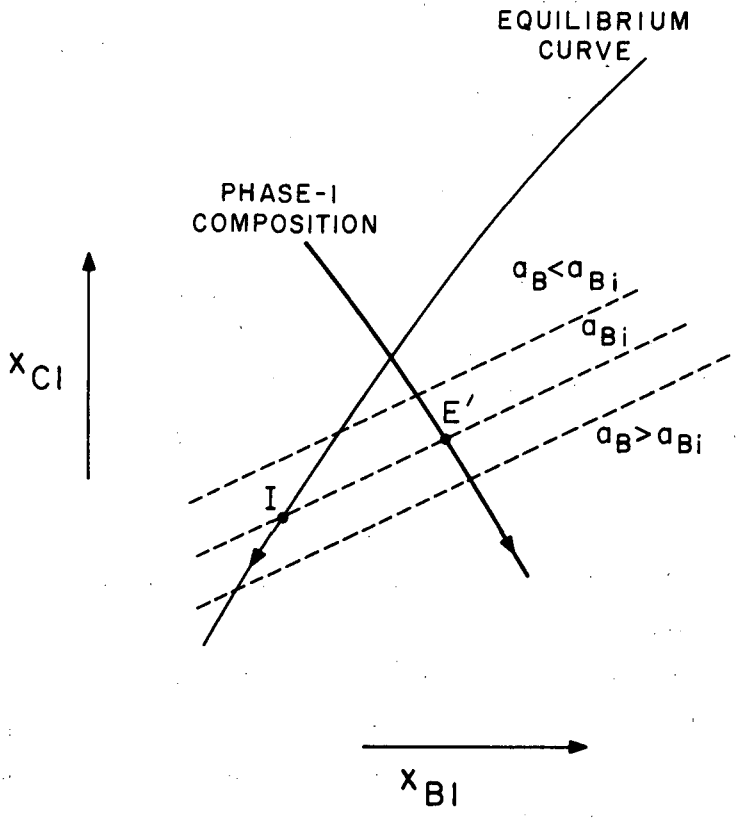

Fig. 8. Activity effect of the minor component on thermodynamic driving potential (phase 1).

the equilibrium curve. Physically this means that for a time after phase 1 enters the column, it is enriched in B; then after it is well inside the equilibrium curve, it rejects B again. This behavior is most easily explained by Fig. 8, which shows the situation that prevails for phase 1 in the forward case.

Point I, in this figure, represents in a general way the equilibrium composition of the interface corresponding to some particular bulk-phase composition of phase 1. The line of constant activity for component B, through point I, lies inside the equilibrium curve in the region where x_C exceeds x_{CI} (that is, where component C is being removed from phase 1). As the bulk composition moves diagonally to the right, the interface and its a_{Bi} line move downward. The intersection E' of the composition line with the a_{Bi} line shows the instantaneous situation where a_{Bl} has overtaken a_{Bi} and the activity gradient is in process of changing sign. In this situation, the system may be said to "register" the attainment of a partial equilibrium; however, the point where it is reached is seen not to lie exactly on the static-equilibrium curve.

A similar explanation applies in the reverse case to component A in phase 2. Here also the concentration change due to the diffusion of A first acts in the same direction as that due to C; then after the composition is appreciably inside the two-phase region, the diffusion of A begins to have an opposite effect.

Figure 1 shows that the slope of the constant-activity lines for B in phase 1 (and A in phase 2) is quite steep, and this means that the partial-equilibrium point actually will lie quite close to the equilibrium line. However, the composition must be inside the partial equilibrium before back diffusion of B can begin to compensate for forward diffusion of C.

A minor diffusional effect of component A appears to reinforce the depletion of C (for forward extraction, in phase 1). Under the conditions assumed for the calculation, interfacial resistance is neglected, and phase 1 is regarded as a source and sink of component A, with the diffusion of A to or from the interface being insensitive to the apparent driving potential. Thus, under this particular assumption, the rate of diffusion of A is determined entirely by its driving potential

between the equilibrium interface and the bulk of phase 2. As the activity of A in phase 2 is always less than the interface value, the diffusion of A is into phase 2. Its direction is such as not only to enhance the crossing-over in phase 1, but also to increase the likelihood of a crossing-over in phase 2. Since the composition of phase 2 always remains at some distance from the equilibrium curve, this effect can be viewed as a secondary one.

As a primary conclusion, it is fair to say that the solute depletion (or solute enrichment) effect is the most important one and is the main cause of crossing-over into the metastable region. The behavior of this ternary system may be compared to that of a binary system undergoing crystallization. The temperature coordinate in binary behavior is analogous to the C-component coordinate in the ternary system. Abstraction of C, like lowering of temperature, carries the system from an undersaturated to a supersaturated condition, after which diffusion toward the equilibrium is counterbalanced by further C abstraction or temperature lowering. The equilibrium (for that particular phase) thereafter is always approached from the supersaturated side.

Since the approximations in our calculation of driving potentials appear to be comparable in their effect to a change in the numerical value of one or another of the mass-transfer coefficients, these approximations are believed to be without effect on the over-all conclusions reached: first, a crossing-over will generally occur in a phase for which the solute-depletion slope is steeper than the constant-mole-ratio slope (for the carrier and the minor component in the phase). Second, decrease in the mass-transfer coefficient for the minor component in the phase involved will cause the concentration profile to deviate more widely from the equilibrium line.

Influence of the Mass-Transfer Coefficients

As explained in an earlier paragraph, the present calculations are based on the assumption that the interface is in equilibrium. This leaves three independent mass-transfer-coefficient ratios k_{C2}/k_{C1}, k_{B1}/k_{C1}, and k_{A2}/k_{C1} to be specified, and these were each varied so as to investigate their influence on the position of the concentration path.

The two remaining ratios, k_{A1}/k_{C1} and k_{B2}/k_{C1} were taken as dependent variables; their values, computed from the known values of Δn_A and Δn_B by mass-transfer relations similar to Eqs. (35) and (36), are reported in Table V. Besides the starting and end values of these ratios, Table V also gives extreme values for k_{B2}/k_{C1} and k_{A1}/k_{C1}. For the latter, the extreme value occurs essentially at the "knee" of the curve for phase 1; that is, at the point where x_A in that phase goes through a minimum.

From the shape of the graph, we note first that k_{C1} and k_{C2} work together to produce a transfer of component C. With $k_{C2}/k_{C1} < 1$, the restoring potentials for components A and B become relatively larger, and static equilibrium is more nearly approached. Because the effects of k_{C1} and k_{C2} do combine, the influence of the coefficients k_{A2} and k_{B1} is better explained by referring them to an over-all mass-transfer coefficient k_{OC}. (Effectively, k_{A2} and k_{B1} are also over-all coefficients). The over-all coefficient for component C is given by

$$\frac{1}{k_{OC}} = \frac{1}{k_{C1}} + \frac{1}{mk_{C2}} \quad . \tag{40}$$

In this relation, m is the distribution coefficient $(x_{C2}/x_{C1})_{eq.}$, whose mean value calculated from the equilibrium curve is 0.460. With $k_{C1} = 1$, and k_{C2} takes the values 2.0, 1.0, or 0.5, the over-all mass-transfer coefficient k_{OC} equals 0.479, 0.315, or 0.187, respectively.

Comparing Run 2 of Fig. 3 with Run 4 in Fig. 4--both having a high ratio of k_{B1}/k_{OC}--we find the profile close to equilibrium in phase 1. For phase 2, the ratio k_{A2}/k_{OC} governs, since the values are different in Runs 2 and 4, and the curves are different. Similarly, comparing Run 3 of Fig. 3 with Run 5 of Fig. 4, we conclude that a high ratio of k_{A2}/k_{OC} carries the profile close to equilibrium in phase 2. For phase 1, the ratio of k_{B1}/k_{OC} governs, since with different values, the curves are different.

The effect of k_{A2}/k_{OC} can be explained as follows: For phase 2, diffusion of A from phase 1 to phase 2 has the effect of pulling the concentration profile toward the equilibrium curve (whereas diffusion of C in the same direction pulls the profile away from the equilibrium curve). While the effect of A is not large enough to balance completely the effect of C, it does serve to determine how closely the profile for phase 2 will approach the equilibrium curve. For phase 1, the effect of k_{B1}/k_{OC} on the concentration path is consistent with having the diffusion of B oppose the diffusion of C and pull the concentration path back toward the equilibrium curve, when the composition is appreciably inside the two-phase region (as was discussed in the preceeding section).

There is a slight indication from Tables V and VI that a higher value of the second ratio (k_{A2}/k_{OC} for phase 1, k_{B1}/k_{OC} for phase 2) carries the curve slightly farther from equilibrium. However, not all runs give results corresponding to this indication. In any event, any such effect is secondary and very small.

Numerical Values of the Unspecified Coefficients

Table VII shows that the mass-transfer ratios k_{A1}/k_{C1} and k_{B2}/k_{C1} may be either negative or positive during the extraction run. Negative values can be explained by considering cross-product transport which results from the diffusion of other species. For a typical run, Table VII shows the concentration values that correspond to $k_{B2}/k_{C1}=0$. In calculating the contribution of cross-product terms to k_{B2}, it is reasonable to assume that the cross-product transport due to diffusion of A is negligible, because the driving potential for A is small and theoretically the cross-product coefficient (k_{AB2}) is also small. Thus, from relations similar to Eq. (24) we can compute the relative magnitude of k_{CB2}. As N_B is equal to zero at this point, we have

$$\frac{k_{CB2}}{k_{BB2}} = -\frac{\Delta a_{B2}/\gamma_{B2}}{\Delta a_{C2}/\gamma_{C2}} = 1.10$$

This shows that the k_{A2}/k_{OC} and k_{B1}/k_{OC} ratios, which apply here

Table VI. Effect of mass-transfer-coefficient ratios on exit concentration of component A in phase 2.

Run No.	k_{A2}/k_{OC}	k_{B1}/k_{OC}	$(x_A)_{2\ out}$
4	21.39	10.69	0.0171146
9	10.69	21.39	0.01722185
5	8.35	4.17	0.017292
3	8.35	1.04	0.017035
11	4.17	8.35	0.016990
1	3.17	3.17	0.016222
6	2.67	1.34	0.015492
8	1.34	10.69	0.01420
2	1.34	3.67	0.01380
7	1.04	0.52	0.01215
10	0.52	1.04	0.008855

Table VII. Concentration values and driving potentials which correspond to $k_{B2}/k_{C1} = 0$ for Run 1 (a "1-1-1" run)

Component	Coexisting compositions		Net movement[a]	Driving potentials and activity coefficients				Mass-transfer coefficients
				Phase 1		Phase 2		
	Phase 1	Phase 2		$a_1 - a_i$	γ_1	$a_i - a_2$	γ_2	
C	0.2392	0.0738	+	+0.01966	1.410	+0.058	3.483	
A	0.7285	0.0148	+	-0.01729	1.0775	+0.0606	49.80	$k_{A1}/k_{C1} = 0.0761$
B	0.0323	0.9114	+	0	28.10	-0.0185	1.015	$k_{B2}/k_{C1} = 0$

[a] Transfer from phase 1 to phase 2 is denoted by +.

and have been assumed to be constant, can lead to a cross-product diffusion coefficient that is not small compared to the principal term, but is at least of a reasonable order magnitude. (It is not likely that the A-B cross-product term for phase 2 could contribute enough diffusion of B to reduce the apparent magnitude of k_{CB2}; the driving potential for A in this phase, although in the same direction as for C, is only about 0.07 times the potential for C.)

The same arguments can be applied to k_{CA1}/k_{AA1}. This ratio changes in sign at $x_{C1} = 0.290$ and $x_{C2} = 0.096$. The relative magnitude of k_{CA1}/k_{AA1} is then equal to 0.028, which agrees more closely with our qualitative expectations.

As a general conclusion we can say that in the range where the two ratios are negative, the cross-product diffusion of A induced by C is large enough to override the direct coefficient and lead to the effective negative value.

Calculations of the Number of Transfer Units

Extraction-tower performance is usually characterized by quantities first introduce by Chilton and Colburn and named by them "number of transfer units" (NTU) and "height of a transfer unit" (HTU). These quantities can be defined for either phase 1 or phase 2, and on the basis of either a single-phase resistance or an effective over-all resistance. They are related to column height in the following way:

$$\begin{aligned}\text{Height of column} &= (\text{function of mass-transfer coefficients}) \\ &\times (\text{function of separation performance}) \\ &= (\text{HTU})\,(\text{NTU}). \end{aligned} \tag{41}$$

Here HTU has dimensions of length, while NTU is dimensionless; within this restriction, the definitions of the two must be compatible but are somewhat arbitrary. The usual practice is to define the NTU value for a particular phase as

$$(\text{NTU})_{ij} = \int_{(x_{ij})_{in}}^{(x_{ij})_{out}} \frac{d(\text{moles component i extracted from phase j})}{\text{driving potential for component i in phase j}}, \tag{42}$$

with the driving potential known as a function of the extent to which extraction has proceeded. Here, where the flowrate is not constant, the number of transfer units for component C in phase 1 can be defined as

$$(NTU)_{OC1} = \int_{(x_{C1})_{in}}^{(x_{C1})_{out}} \frac{\gamma_{C1}\, dx_{C1}}{a_{C1} - a_{C2}} \cdot \frac{F_1}{(F_1)_{in}} \quad . \tag{43}$$

The results of this investigation enable us to determine the effect of concentration profile upon NTU value. For the usual equilibrium-curve approximation to the profile, $F_1/\left[x_{C1} - (x^*_{C1}\, \gamma^*_{C1}/\gamma_{C1})\right]$ was plotted against x_{C1} and was integrated numerically or graphically between the effective value of $(x_{C1})_{in}$ (equilibrium-curve value, in this case 0.291) and $(x_{C1})_{out}$ (here 0.056).

The corresponding NTU values for the computed concentration profiles were evaluated as part of the computer calculation. The relation used was

$$\delta(NTU)_{OC1} = \frac{k_{OC}}{k_{C1}} \cdot \frac{\gamma_{C1}\, \delta x_{Ci}}{a_{C1} - a_{Ci}} \cdot \frac{F_1}{(F_1)_{in}} \quad , \tag{44}$$

where the γ, a, and F values were all evaluated at the start of each slice, and the increments were added cumulatively. This calculation is identical in its result to using $a_{C2} - a_{C1}$ as the driving potential and omitting the mass-transfer-coefficient ratio. The following values of over-all NTU for component C relative to phase 1, were obtained:

Equilibrium-curve approximation	3.85
Run 1 (intermediate approach to equilibrium curve)	3.66
Run 7 (furthest departure from equilibrium curve in both phases)	3.75
Run 5 (near approach to equilibrium curve in both phases)	3.82
Run 2 (near equilibrium curve in phase 1, far from equilibrium curve in phase 2)	4.29
Run 3 (near equilibrium curve in phase 2, far from equilibrium curve in phase 1)	3.53.

Comparing Run 5 with the equilibrium-curve approximation, we see that the NTU values are almost the same, because the concentration path for Run 5 is close to the equilibrium curve. For the other values, when the concentration path for phase 1 is far from equilibrium, the NTU value may either drop or rise, depending on whether the concentration path is mainly inside or mainly outside the equilibrium curve. On the other hand, when the concentration path for phase 2 is far from equilibrium, the value for the NTU rises. Thus we often deal with two opposite effects, and for intermediate cases we may get a partial compensation.

The effect just described can be explained with the help of the constant-activity line for component C, shown in Fig. 1. With reference to a material-balance line drawn through an exterior "operating point" (which will be in nearly the same position for both the equilibrium-curve treatment and any concentration-profile calculation), we find $a_{C1} < a_{C1E}$ when the concentration profile for phase 1 is inside the two-phase region. Thus the driving potential $(a_{C1} - a_{C2})$ is then smaller than the driving potential for the equilibrium-curve approximation, and the contribution of phase 1 to the NTU will be higher. When the concentration profile for phase 1 lies outside the equilibrium curve, the driving potential is larger, and the NTU contribution will be less. In the same manner, the constant-activity lines for component C show that when the concentration path for phase 2 is outside the two-phase region, a_{C2E} is less than a_{C2}. This leads to a smaller driving potential for $a_{C1} - a_{C2}$, and a higher NTU value than that of the equilibrium-curve approximation.

Run 2 shows the greatest rise in the NTU, resulting from increases due to both phase 1 and phase 2. Run 3 shows the greatest drop; here the drop from phase 1 outside the equilibrium curve overshadows the later rise due to phase 1 inside (and also the rise due to phase 2). Runs 1 and 7 reflect somewhat similar behavior.

Start-up History for a Run

We need now to determine from qualitative considerations whether a column could arrive at the concentration profiles computed numerically for it. The composition at several heights in the column for a sequence of times after start-up will be shown to approach the ultimate steady-state concentration profile in the manner indicated on Figs. 9 and 10.

Our qualitative considerations will be applied to an extraction column where the two streams flow countercurrently, the solvent being introduced at the bottom and the feed at the top. We consider the two cases, where either phase 1 or phase 2 is continuous, to see how the concentration varies with time in both cases.

Phase 1 continuous. This case is illustrated in Fig. 9. Let the column be filled with phase 1, flowing at its steady-state flow rate. Phase 2 is then introduced dropwise at its respective flow rate. The first drops of phase 2 will be completely dissolved by phase 1. We start our time scale at t_0, at which the discontinuous phase first begins to leave the column. Because of a higher affinity for component B, the concentration profile for phase 1 (at t_0) crosses the equilibrium curve earlier than the steady-state curve, and phase 1 throughout contains more of C than it would in the steady state. The first drops of phase 2 that do survive effect a maximum extraction of component C, and this larger extent of extraction intensifies the crossing-over effect so that the t_0 curve for phase 1 is carried further inside the equilibrium curve than in the steady-state. As extraction continues, phase 1 (after having entered the column) comes in contact with a phase 2 that contains gradually more of A and C. Thus the transfer of B into phase 1 and of C into phase 2 becomes less rapid, and the concentration profiles approach the steady-state values. On the same graph we have also plotted the concentration lines for five different heights in the column. All these profiles start on the concentration curve corresponding to t_0; for simplicity the profiles for times between $t = 0$ and $t = t_0$ have been omitted.

Phase 2 continuous. When phase 2 is continuous (Fig. 10), the behavior of the column can be described in quite similar terms. Into phase 2 flowing at its steady-state flow rate, phase 1 is introduced dropwide at its respective flow rate. The first drops of A will be dissolved by phase 2; then, when the drops survive, they undergo maximum extraction of component C, losing C much more rapidly than they can gain B. Thus the concentration profile (for phase 1) corresponding to t_0 crosses the equilibrium curve later than the steady-state profile. As initially phase 2 is enriched rapidly in A, its concentration profile is carried closer to the equilibrium curve than in the steady state.

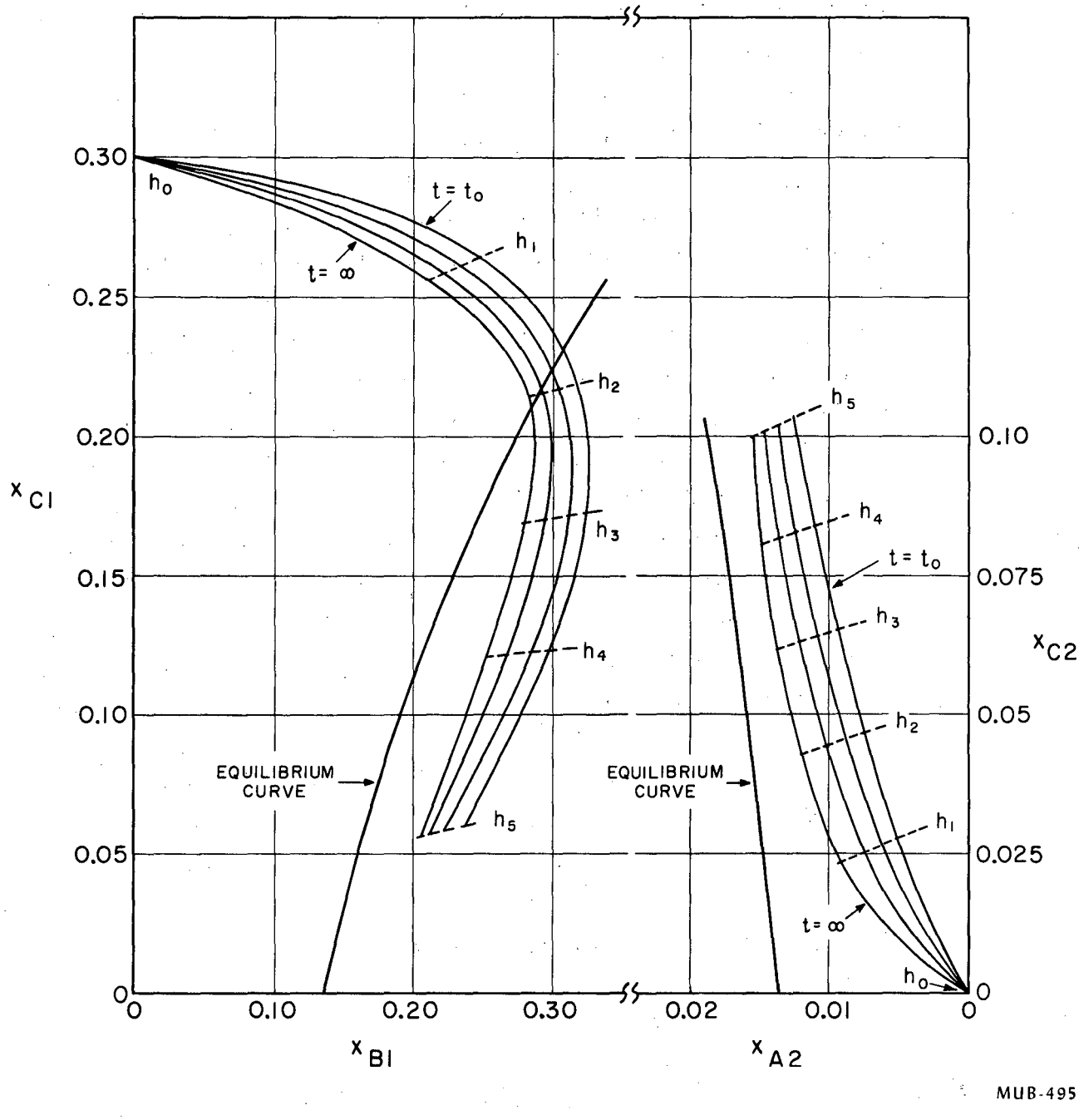

Fig. 9. Start-up behavior of an extraction column, with phase 1 continuous.

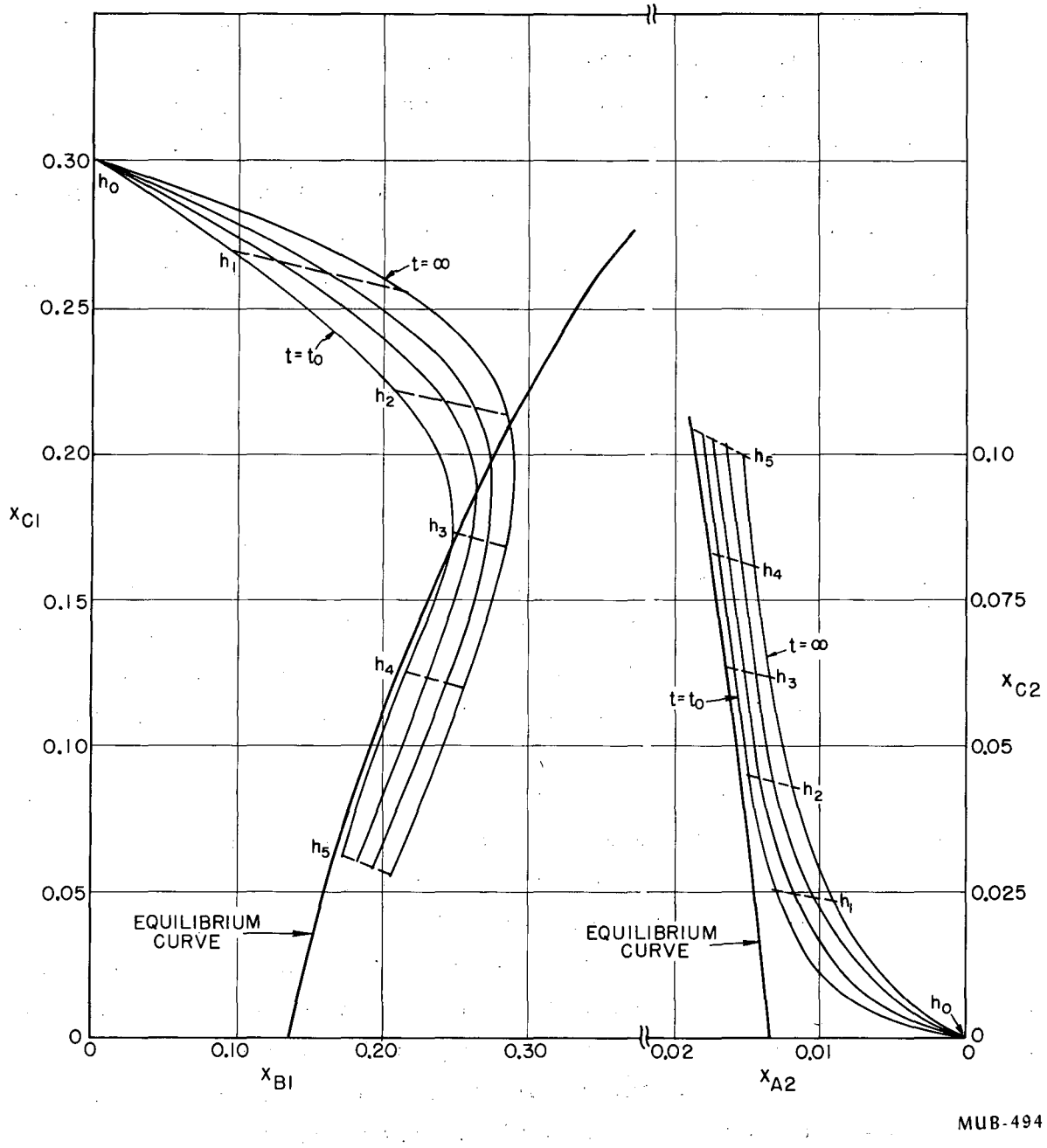

Fig. 10. Start-up behavior of an extraction column, with phase 2 continuous.

However, diffusion of C always keeps phase 2 from crossing the equilibrium line. As extraction continues, the concentrations at each point in the column change steadily toward the steady-state values.

These qualitative considerations show that as the extraction proceeds, the unsteady concentration profiles in both cases can approach the steady-state ones as a limit. It is interesting to notice that the same factors that cause the concentration profiles to cross the equilibrium line in the steady state also serve to bring about this effect at start-up, but at a different point in the column.

CONCLUSIONS

From the results of this investigation one can draw the following conclusions:

a. Activity differences as driving potentials give a much more realistic picture than the usual concentration driving potential. For very accurate calculations, one could replace the bulk activity coefficient in the mass-transfer equation by a suitable mean value and could also take into account the individual values of the cross-product coefficients for mass transfer.

b. Based on the theory that is presented here, the concentration path does not approach the equilibrium curve instantaneously and then follow it, as is usually assumed. Instead it may actually cross the equilibrium curve for one phase while staying away from it for the other.

c. The direction of diffusion of the transferring component (C, in our study) is the main factor that determines whether a phase will cross the equilibrium line. For the usual case where the equilibrium shows an increase of the minor component in each phase as the transferring component is augmented, the phase that loses the transferring component is the one whose composition tends to cross the equilibrium curve.

d. The distance between the calculated concentration paths and the equilibrium line depends on the mass-transfer coefficients. The larger the over-all coefficient for component A, the nearer the phase-2 curve is to the equilibrium curve; the larger the over-all coefficient for component B, the nearer phase 1 approaches the equilibrium curve.

e. The NTU values depend largely on the separation between the calculated concentration path and the equilibrium curve, in each phase. For extreme cases the number of transfer units calculated from the exact concentration path can differ as much as 10% from that calculated by the usual standard method.

f. Experimental verification of the calculated effects is needed. If the predicted effect is real, two-component analysis should replace single-component analysis of interior or terminal samples from operating extraction equipment involving ternary systems.

ACKNOWLEDGMENTS

The authors are deeply grateful to the Lawrence Radiation Laboratory and the United States Atomic Energy Commission for financial support to Alphonse Hennico; and to the Miller Institute of Basic Research in Science at this University for support to Theodore Vermeulen, during the course of this research.

Professors R. Defay (University of Brussels, Belgium), J.H. Hildebrand, J.M. Prausnitz, and D.R. Olander participated at various times in extensive basic discussions on theoretical background.

This work was performed under the auspices of the U. S. Atomic Energy Commission.

NOTATION

A	:	Margules constant, for Eq. (1)
a	:	activity
B	:	length coordinate, cm
b	:	length coordinate, cm
c	:	concentration, moles/liter
D_0	:	diffusion coefficient at infinite dilution, cm^2/hr
D	:	modified diffusion coefficient (Eq. 20)
D	:	modified diffusion coefficient (Eq. 25)
$\mathscr{D}$	:	diffusion coefficient multiplying μ gradient (Eq. 13a)
d	:	differential operator
F	:	flowrate of a phase, g-moles/hr
f	:	function of
HTU	:	height of a transfer unit, cm
h	:	height of a differential section in the extraction column, cm
k, k'	:	mass-transfer coefficient, (g-moles)/(hr cm^2)(g-moles/liter)
(ka)	:	product of mass-transfer coefficient and interfacial area per unit volume (liter)/(hr cm^3)
M	:	a function of Margules constants for a ternary system (Eq. 4)
m	:	distribution coefficient, $(x_{C2}/x_{C1})_{equil.}$
N	:	number of moles transferring per unit area per unit time
NTU	:	number of transfer units
n	:	number of moles transferred between phases per unit time
R	:	universal gas constant, (cm)(g)/g-mole ^oR
T	:	absolute temperature, ^oR
t	:	time
V	:	a variable
x	:	mole fraction
z	:	a variable

Greek Letters:

α	:	numerical constant(Eq. 5)
β	:	numerical constant (Eq. 6)
γ	:	activity coefficient, a_{ij}/x_{ij}

∂ : partial differential operator

δ : increment

μ : chemical potential

η : viscosity

Σ : summation

Subscripts:

A, B, C : components of the ternary system

E : equilibrium-line value

i : interphase

j : component

O : over-all

p : phase

1 : a phase rich in A

2 : a phase rich in B

Superscript:

* : equilibrium

BIBLIOGRAPHY

C1 T. H. Chilton and A. P. Colburn, Ind. Eng. Chem. 27, 255 (1935).

C2 A. P. Colburn and D. G. Welsh, Trans. Am. Inst. Chem. Engrs. 38, 143 (1942).

D1 P. V. Danckwerts, Ind. Eng. Chem. 43, 1460 (1951).

D2 L. A. Darken, Metals Technology 15, T. P. 2311 (1948).

D3 K. G. Denbigh, Thermodynamics of the Steady State (Methuen and Co., London, 1951, Chaps III and IV.

G1 J. Willard Gibbs, Collected Works, Vol. 1 (Yale University Press, New Haven, Conn., 1906), pp. 105 to 115.

G2 S. R. de Groot, Thermodynamics of Irreversible Processes (North Holland Publishing Co., Amsterdam, 1951), Chap. VII.

H1 R. Haase, Thermodynamik der Mischphasen mit einer Einführung in die Grundlagen der Thermodynamik (Springer Verlag, Berlin, 1956, pp. 151 to 183.

H2 A. E. Handlos and T. Baron, A. I. Ch. E. Journal 3, 127 (1957).

H3 R. Higbie, Trans. Am. Inst. Chem. Engrs. 31, 365 (1935).

H4 J. H. Hildebrand and R. L. Scott, The Solubility of Nonelectrolytes (Reinhold Publishing Corporation, New York, N. Y. 1950), Chap. VII.

K1 G. Kortüm and H. Bucholz-Meisenheimer, Die Theorie der Destillation und Extraktion von Flüssigheiken Springer Verlag, Berlin, 1952, pp. 22 to 32.

K2 J. P. Kuenen, Theorie der Verdampfung und Verflüssigung von Gemischen und der Fraktionierten Destillation (Verlag, G. A. Barth, Leipzig, 1906), pp. 68 to 69.

L1 G. S. Laddha and J. M. Smith, Chem. Eng. Progr. 46, 195 (1950).

O1 J. B. Opfell and B. H. Sage, Ind. Eng. Chem. 47, 918 (1955).

P1 I. Prigogine and R. Defay, Treatise on Thermodynamics, (Longmans-Green Publishing Co., New York, N. Y., 1954) Chap. XVI.

S1 T. K. Sherwood and R. L. Pigford, Absorption and Extraction, (McGraw-Hill Book Co., New York, N. Y., 1952) p. 415.

S2 A. S. Smith and T. B. Braun, Ind. Eng. Chem. 37, 1048 (1954).

S3 A. E. Stearn, and H. Eyring, J. Phys. Chem. 44, 955 (1940).

T1 R. E. Treybal, Liquid Extraction, McGraw-Hill Book Co., New York, N. Y., p. 131.